



RAPID SOLIDIFICATION OF HYPERMONOTECTIC Al-In ALLOYS

S. Umamaheswara Rao and G.V.S. Sastry

*Centre of Advanced Study, Department of Metallurgical Engineering,
Institute of technology, Banaras Hindu University, Varanasi-221005, India*

ABSTRACT

Hypermonotectic Al-12at%In foils have been produced by melt spinning. The resulting microstructure has been examined by transmission electron microscopy. The rapidly solidified hypermonotectic alloy basically exhibits a microstructure consisting of Al matrix with trimodal distribution of In rich liquid. These distributions are large droplets of 0.2-2 microns size that resulted from phase separation, 40 to 120nm size particles from monotectic reaction and a modulated structure with approx. 30nm wave length from spinodal decomposition in the solid state. These results have been compared with earlier results obtained for the rapidly solidified monotectic Al-In alloys.

1. INTRODUCTION

'Rapid solidification' of Al-In alloy (liquid immiscible system) exhibiting monotectic reaction is an interesting topic among researchers¹⁻⁶ for more than 3 decades. Rapid solidification produced nano In particles¹⁻³, nano-composites⁷ in monotectic systems. The first ever rapid solidification (gun quenching) of monotectic Al-In alloy (4.7at%In. See Fig.1) was carried out by Ojha and Chattopadhyay [1] and given various possibilities to explain the resultant microstructure. Chatopadhyay et al^{8,9} have further described the observed microstructures speculating a metastable solid state miscibility gap in the rapidly solidified monotectic Al-In alloy. The present study concentrates the rapid solidification of the hypermonotectic Al-In alloys to compare the effect of increase in In content on the structure of this alloy. A hypermonotectic Al-12at%In composition has been chosen as it should not be far away from the monotectic composition of 4.7at%In.

2. EXPERIMENTAL PROCEDURE

Al and In of five nines purity were used for making the Al-12at%In (36.72wt%In) alloy for this investigation. The respective amounts of metals were carefully weighed and melted in an alumina crucible. Argon gas was purged through silica glass tube in which alumina crucible with the sample was kept. The melting was done by induction furnace. First the Al was melted and superheated it 100-125°C above immiscibility dome i.e., to 880°C and then In was added. The superheat of the Al bath was kept on the higher side to avoid the chilling of the bath by the addition of In down to immiscibility dome which leads layer formation immediately. The melt was kept for 1-2 min at this temperature to homogenize the alloy. On slow cooling the alloy was stratified into two layers.

Stratified alloy was not used for melt spinning. Sample for melt spinning has been made separately in 2gm individual batches. The alloy was melted in-situ in graphite crucible of the melt spinning apparatus. The homogenized alloy melt was ejected from a temperature of approximately 780°C through 0.5 mm nozzle of the graphite crucible. Wheel speed maintained

was 45m/s. Resultant foils dimensions were of 0.4 -3mm width and 0.5-7mm length. Many areas of the foils were sufficiently thin for the observation under TEM without any specimen preparation. The thin foils were observed under JEOL-200CX TEM operated between 120-160KV.

3. RESULTS

3.1 Microstructure of as-cast material

The microstructure of the as-cast Al-12at%In alloy consists of 2 clear layers as shown in Fig.2a. Top Al rich layer exhibits a microstructure corresponding to monotectic reaction (Fig.2b.). The bottom layer consists of eutectic reaction (Fig.2c). The bottom layer also has pro-eutectic Al dendrites growing up toward Al rich layer (Fig.2d) because of the primary heat extraction by highly conducting Al.

3.2 Microstructure of rapidly solidified foils

TEM studies of samples have shown a distribution of droplets of dark contrast in a bright matrix. They have shown a continuous white phase and 3 types of dark droplets in and or above the white matrix surface. A typical microstructure is shown in Fig.3. One size range is 200nm-2 μ m, second is thin layer of 40-120nm and third is of spinodal decomposition with an average wave length of 30nm which is shown in Fig.4. The bigger sub-micron size droplets are in a state of coalescence at some places as in Fig.3. Cellular structure of the grain boundaries can also be seen much clearly.

4. DISCUSSION

4.1 Droplet formation by phase separation

During cooling, the first step that occurs in a hypermonotectic alloy is the liquid phase separation into L_1 and L_2 . Suppression of nucleation is difficult in hypermonotectic alloys^{2,10} because positive enthalpy of these immiscible phases continues even to low temperatures and even high undercooling rates may not avoid the repulsive interactions between the dissimilar phases. So, L_2 , being minority phase, nucleates first¹¹, and coagulates until it solidifies. Coagulation can be seen from the Fig.3. The collision and coagulation studies were made in detail¹². Also in the present study, varied size of ranges the droplets from phase separation are observed throughout the microstructure. Zhao et al¹³ made modeled the repeated nucleation of minority liquid phase in the undercooled liquid (See Fig.5). According to both of them, it can be understood that the droplets nucleated initially can coagulate much more than that nucleated later and produce bigger sizes. It can also be understood that the micron-size and sub-micron size droplets are not properly wetting the surface of the matrix which is one of characteristic of immiscible phases.

4.3 Droplet formation by monotectic reaction

The matrix or liquid L_1 , during continued cooling, rejects In atoms until it reaches the monotectic, the reaction which gives L_3 and L_4 . Nucleation of Al grains starts at this temperature on the wheel surface and they grow laterally to form columnar grains. The nucleation of the L_4 droplets will take place either homogeneously ahead of Al growth front or heterogeneously in contact with Al interface depending on the contact angle θ at the $S_{Al-L_3-L_4}$ triple point. Nucleation of the L_4 phase has been shown schematically in Fig.6

In the present study, In rich particles resulting from monotectic reaction have exhibited faceting (a characteristic of metastable In') with 40 to 120nm size particles in some regions as shown in Fig.4. This metastable In' phase with FCC crystal structure was observed earlier in the rapidly solidified Al-In alloys^{1-3,15}. The investigators either quenched this alloy directly from liquid or solution treated with/without aging before identifying the metastable In' phase. In our case, without any aging the particles showed faceting under TEM observation, and this faceting is observed to be limited to some areas whereas they appeared to be spherical in some other areas. If we assume the faceting behavior may be due to the heating effect of electron beam in TEM, then it should have extended to all areas of the sample; but it is not so. Further, Zhang et al³ have got the faceting in melt-spun Al – 7wt%In alloys without any aging. So it can be concluded that in this case In' nano particles were resulted by monotectic reaction where the Al growth front is sufficiently slower (although it is very faster than normal solidification) to allow the In droplets to adjust to its minimum energy shape (Truncated octahedron). Ojha et al¹ reported that In' particles adopted hexagonal shapes, whereas the diffraction data of Silcock¹⁵ indicated a nearly spherical shape for the same. These observations are consistent with the truncated octahedron shape of the metastable In', since this polyhedron appears hexagonal when viewed in a <111> projection and is a close geometrical approximation to a sphere as shown in Fig.7.

4.2 Droplet formation by spinodal decomposition

Chatopadhyay et al⁸ explained the modulated structure assuming a solid state miscibility gap considering fcc structure of In' along with the fcc structure of Al. But they have not shown the exact position of this solid state miscibility gap on the phase diagram. With the help of the thermodynamic aspects of the phase diagrams, the solid state miscibility gap has been drawn schematically as shown in Fig.5. The importance of this diagram is that this is the only means, so far, to explain all observed microstructures in this system.

Van Aken et al² identified the Indium rich phase in the modulated structure as metastable In' but no explanation was offered why such type of structure was emanated. So an attempt has been made to expound it. The spinodal decomposition should have occurred near the equilibrium eutectic temperature (429K). This is because the tetragonality of In decreases with increasing temperature¹⁶ from room temperature, and at 408K temperature the ratio of c/a was 1.065 compared to normal ratio of 1.52. The tetragonality of In also decreased by solid solution alloying with metals of valency 3 or less¹⁷. Therefore it can be speculated that a combination of the effects of alloying and temperature might have produced cubic In near the solidification point or eutectic temperature.

5. SUMMARY

The melt spun hypermonotectic Al-12at%In alloy basically exhibits trimodal distribution of In rich liquid in Al matrix. Large droplets of 0.2-2 microns size produced from phase separation by repeated nucleation of the minority phase i.e., L₂. The droplets nucleated first grown to bigger sizes and were coalescing. 40 to 120nm size originated from monotectic reaction exhibiting faceted morphology. Finally, a modulated structure has been observed which has been explained on the basis of a solid state miscibility gap in which In is in metastable fcc form. The modulated structure with 40 to 120nm particles is similar to the earlier results obtained. The experimented undercooling might not suppress nucleation in Al-12at%In alloy.

REFERENCES

1. Ojha S. N. and Chattopadhyay K., Trans. IIM, 31 (1978), 208.

2. Van Aken D. C. and Fraser H. L., Inter. J. Rapid Solidification, 3 (1988), 199.
3. Zhang D.L. and Cantor B., Phil. Mag., A 62 (1991), 557.
4. Guo J, Liu Y, Jia J, Su Y, Ding H, Zhao J, and Xue X, Scripta Materialia 45(2001) 1197.
5. Akihiko Kamio, Shinji Kumai, Hiroyasu Tezuka, Mater. Sci. Engg., A146 (1991), 105.
6. Zhao J.Z. and Ratke L., Materials Letters 38(1999) 235.
7. Chattopadhyay K., Nanocomposites by rapid solidification route, Bull. Mater. Sci., 15 (1992) 515.
8. Chattopadhyay K., Ravi V.A., Ranganathan S., Acta. Metall., 34 (1986) 691.
9. Goswami R., Chattopadhyay K., Mat. Sci. Engg., A179/A180 (1994)163.
10. Cahn J.W., J. Amer. Ceram. Soc., 52 (1969), 118.
11. Ratke L., Diefenbach S., Mater. Sci. and Eng., R15 (1995), 263.
12. Rogers J.R. and Davis R.H., Met. Trans, 21A (1990), 59.
13. Zhao J.Z. and Ratke L., Scr. Mater. 39 (1998) 181.
14. Cahn J. W., Met. Trans., 10A (1979) 119.
15. Silcock J. M., J. Inst. Met., 84 (1955-56), 19.
16. Raynor G. V., Moore A. and Graham J., J. Inst. Metals, 84 (1955-56), 86.
17. Guttman L., Trans. Met. Soc. AIME, 188 (1950), 1472.

NOMENCLATURE

- L_1 – (i) Initial homogeneous liquid and (ii) Al rich liquid after phase separation
 L_2 - Micron size droplets that resulted from phase separation
 L_3 – Al rich liquid that originated from monotectic reaction
 L_4 – In rich droplets of 40 to 120nm that resulted from monotectic reaction
 γ – Interfacial energy
 In' – Metastable In phase (FCC structure)

FIGURES

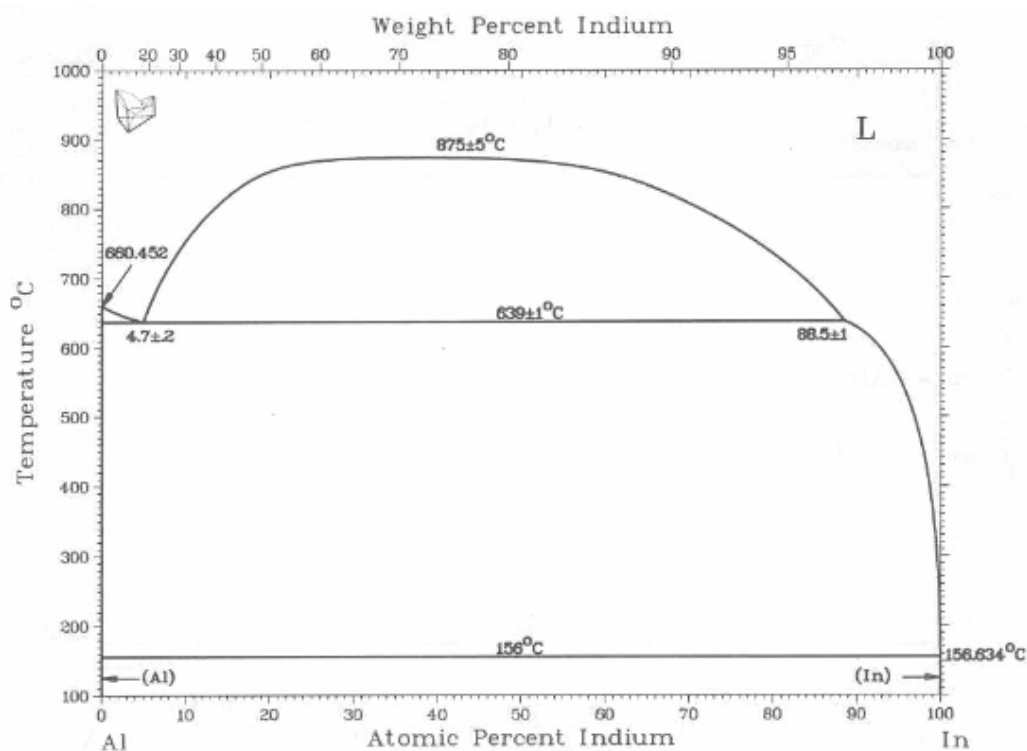


Fig. 1. Al-In Phase diagram [After Murray J. L, Bull. of Alloy Phase Diagrams, 4(3) 1983]

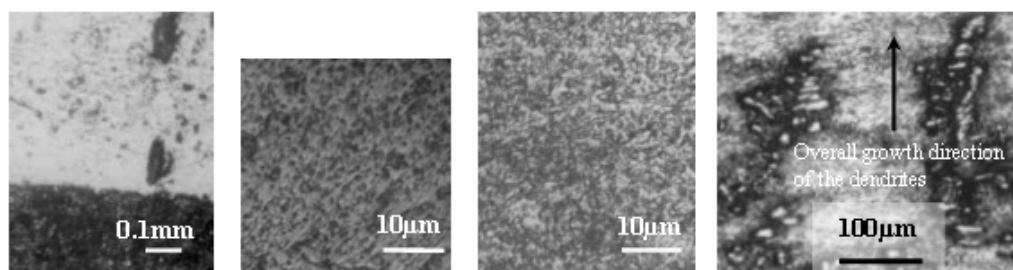


Fig. 2. Optical microscopy of Al-12at%In alloy (a) Stratification (b) monotectic reaction in the top Al rich layer, (c) eutectic reaction in the bottom In rich layer, (d) Pro-eutectic dendrites of Al in the bottom layer. Sample etched in 6% HNO_3 for 6-8 seconds.

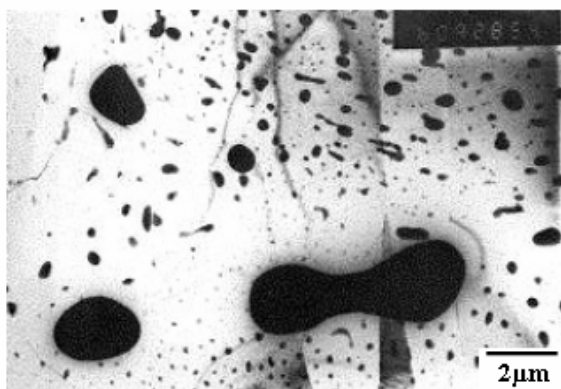


Fig.3. TEM bright field micrograph showing overall distribution of In droplets in Al matrix.

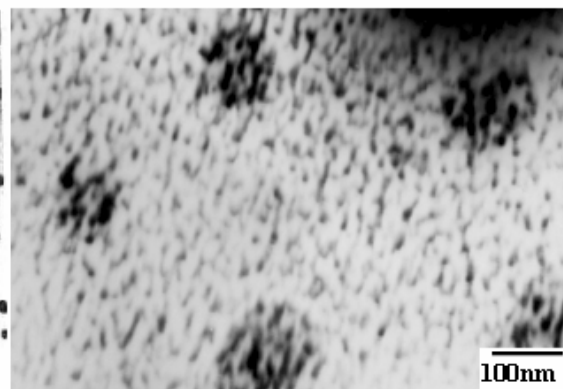


Fig.4. Modulated structure of Al matrix and dark droplets originated from monotectic reaction. (A structure similar to Ojha et al¹)

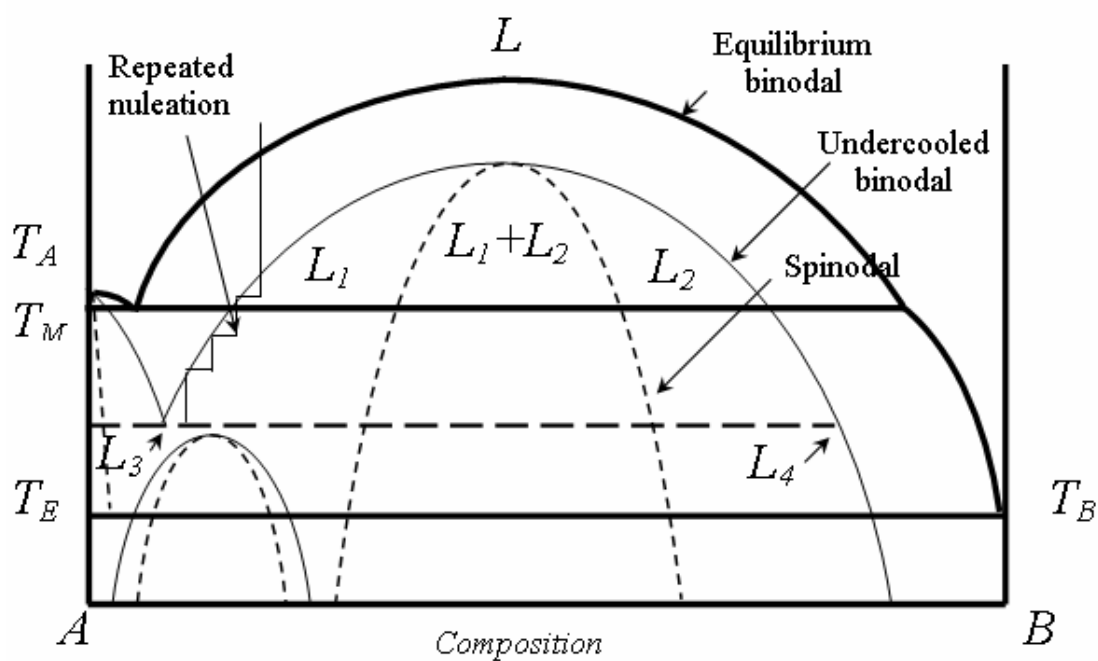


Fig.5 Schematic diagram showing the metastable phase field in the monotectic system

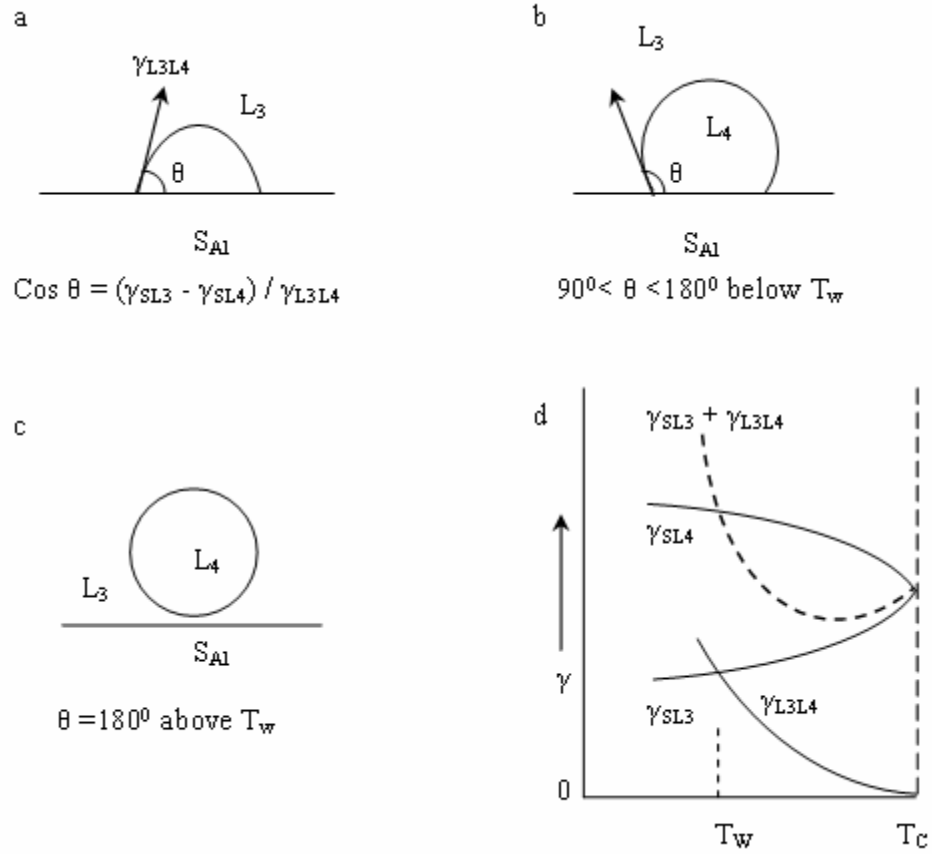


Fig.6. Schematic representation of nucleation of the nano-sized L_4 particles on or ahead of the Al interface: Heterogeneous nucleation with $\theta < 90^\circ$ (a), $90^\circ < \theta < 180^\circ$ (b), homogeneous nucleation with $\theta = 180^\circ$, and variation of interfacial energies with temperature [After Cahn¹⁴] (d).

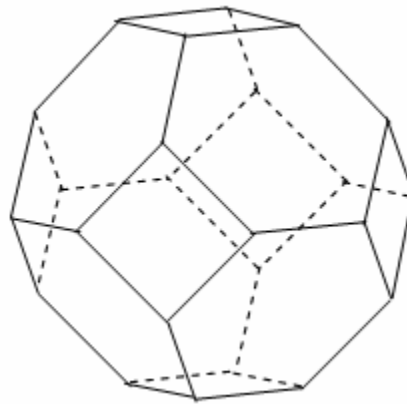


Fig.7. Truncated octahedron shape of metastable In' phase